Desalination and Water Treatment
www.deswater.com
doi: 10.5004/dwt.2023.29548

294 (2023) 233–246
May

High-performance raw biosorbent derived from Algerian Zean oak sawdust for removing methylene blue from aqueous environments

Louiza Sadoun[a,b,*], Karima Seffah[a,c], Abdelbaki Benmounah[a], Abdellatif Zerizer[a], Djamel Ghernaout[d,e]

[a]*Research Unit, Materials, Processes and Environment, M'hamed Bougara University, 35000, Boumerdes, Algeria, Tel.: +213 550 11 66 88; emails: l.sadoun@univ-boumerdes.dz/sadounlouiza@yahoo.fr (L. Sadoun), karimafella@yahoo.fr (K. Seffah), a.benmounah@univ-boumerdes.dz (A. Benmounah), Zerizer_ab@univ-boumerdes.dz (A. Zerizer)*
[b]*Process Engineering Department, Faculty of Sciences, Abdellah Morsli University Center, 42000 Tipaza, Algeria*
[c]*Department of Material Sciences, Faculty of Sciences, University of Algiers 1-Ben Youcef Benkhadda, 16000 Algiers, Algeria*
[d]*Chemical Engineering Department, College of Engineering, University of Ha'il, P.O. Box: 2440, Ha'il 81441, Saudi Arabia*
[e]*Chemical Engineering Department, Faculty of Engineering, University of Blida, P.O. Box: 270, Blida 09000, Algeria, email: djamel_andalus@yahoo.fr*

Received 12 December 2022; Accepted 3 April 2023

ABSTRACT

This work aimed to use Algerian Zean oak (AZO) sawdust in its raw state, without undergoing any physico-chemical treatment, to estimate its efficiency for removing methylene blue (MB), a cationic dye widely used in the textile industry. The physico-chemical properties of the biomaterial were characterized by scanning electron microscopy, Fourier-transform infrared, X-ray diffraction, and Brunauer–Emmet–Teller for measuring its specific surface area. The chemical characteristics of the AZO sawdust surface were further examined by the zero-charge point (pH_{PZC}), iodine, MB numbers, and Boehm titration tests. The batch study was performed by varying parameters such as contact time, particle size, pH, temperature, adsorbent dose, and initial dye concentration. By optimizing these parameters, an adsorption capacity of 52.376 mg/g was attained, at pH = 7 and room temperature, using a dose of 1 g/L AZO at C_0 = 20 mg/L for an equilibrium time of 45 min. The adsorption capacity of the MB is enhanced by increasing the initial dye concentration and the biosorbent dose. The kinetic data were modeled using the pseudo-first-order, pseudo-second-order, Elovich, and intraparticle diffusion models. The results reveal that the pseudo-second-order model better describes the experimental data. Furthermore, the adsorption isotherms well follow the Sips and Langmuir models. The thermodynamic study revealed that the adsorption process of MB on AZO sawdust is a spontaneous, exothermic, and favorable phenomenon. Therefore, AZO sawdust could be considered an efficient biosorbent and a preferred alternative to activated carbon to remove MB.

Keywords: Sawdust; Algerian Zean oak (AZO); Adsorption; Methylene blue (MB); Isotherm models; Adsorption kinetics

1. Introduction

Environmental protection requires special attention to industrial activities that use chemicals in manufacturing. For example, many industrial processes, such as textiles, paper, pharmaceuticals, leather tanning, and cosmetics, use synthetic chemicals like dyes [1]. These are sometimes discharged into the receiving environment without prior treatment, leading to dangerous environmental toxicological effects [2,3]. Moreover, due to their complex molecular

* Corresponding author.

structures and high resistance to temperature, light, and various oxidizing agents, their bioaccumulation in living beings develops, leading to many harmful effects on human health [4]. Among these dyes, methylene blue (MB) is a cationic dye widely used, especially in the textile industry; it can also be used as a redox indicator, antiseptic to treat wounds, and a histological tracer [5].

Today, for removing dyes and reducing their impact on the environment, various methods are adopted including coagulation–flocculation [6], membrane filtration, and oxidation processes [7,8], especially photocatalysis that has shown promising results and proven to be effective in removing organic pollutants and non-biodegradable substances from wastewater [9]. However, most of these methods are expensive, require a lot of energy, produce vast amounts of sludge, and generate wastes that are sometimes more toxic than the original products [10]. Adsorption remains the most effective method, which gives promising results [11]. As a result, over the past few decades, there has been an increasing emphasis on implementing new biomass-based adsorbents, many of which are agricultural by-products and gaining increasing attention in wastewater management due to their availability and low cost [12]. In addition, they have proven to be very effective in removing dyes. Several types of biomaterials have been used, such as *Aloe vera* [13], coffee husks [14], argan nutshell [15], and corn cob [16]. One of the most promising adsorbents is sawdust, which is widely used for removing various organic pollutants, such oils, dyes, and heavy metals [17–19]. A new natural biodegradable adsorbent-based Algerian Zean oak (AZO) sawdust has been developed in this context. It is a product rejected in huge quantities by sawmills and wood processing.

The main objective of this study is to valorize a natural material of recovery derived from a precursor of forest waste, namely the AZO sawdust, a by-product of wood industries very abundant in Algeria. It is an inexpensive waste, ecological, and primarily available. This biomaterial is used in its native state without any physical or chemical activation treatment to eliminate MB, a species found in large quantities in wastewater from the textile industry, which can cause substantial environmental problems. The biocomponent was prepared and characterized using Fourier-transform infrared (FTIR) spectroscopy, X-ray diffraction (XRD), scanning electron microscopy (SEM), and N_2 adsorption–desorption isotherm (that is, Brunauer–Emmet–Teller, BET) The parameters influencing this biosorption were optimized, followed by the determination of MB removal kinetics, isotherm models, and thermodynamic parameters. The high availability of these by-products makes them suitable for use as biosorbents, offering an economical, sustainable, and efficient biosorption material for the remediation of dye-laden effluents.

2. Materials and methods

2.1. Chemical reagents

All reagents and solvents used in this study were of high purity and analytical grade. MB, Na_2CO_3, and $HNaCO_3$ were purchased from Sigma-Aldrich (USA), NaOH and HCl (37%) were obtained from Merck Chemical Company (Germany). MB was chosen as an adsorbate model because of its availability and wide use in the textiles' industry. It is a cationic dye supplied by Aldrich (chemical formula $C_6H_{12}ClN_3S$, molecular weight 319.85 g/mol) and used without further purification. Its different solutions were prepared by dissolving the required quantities of MB in distilled water.

AZO sawdust was collected from northern Algeria's Hadjout (Tipaza) sawmill. First, it was washed several times with tap and distilled water to remove any unwanted material (dust, impurities) until pH ~ 7 was achieved. Next, the clean sawdust was air dried at room temperature for two weeks, then in an oven at 70°C until it attained a constant weight. Finally, the adsorbent material was crushed and sieved to obtain particles of different sizes. The fine powder thus obtained was stored in small hermetically sealed boxes ready for adsorption studies.

2.2. Chemical analysis

The moisture content, H (%), was determined by drying the adsorbent in an oven at 105°C until its weight remained constant. Then, it was calculated using Eq. (1):

$$H(\%) = \frac{m_0 - m_1}{m_0} \times 100 \quad (1)$$

where m_0 (g) and m_1 (g) are the adsorbent masses before and after drying, respectively.

The ash content C (%) was evaluated by the difference in the mass of the biosorbent before and after calcination at 800°C.

The pH of the zero-charge point (or pH_{PZC}) representing the pH value for which the net charge of the adsorbent surface is zero, was determined using the procedure described by Badis et al. [20]. The Boehm titration method was used to identify the number of acidic and basic functional groups on the biomaterial's surface. For this purpose, 0.1 g of powder was placed in a series of Mayer flasks containing 50 mL of 0.1 N Na_2CO_3, $HNaCO_3$, NaOH, and HCl, to determine the nature of the surface functions (carboxylic, phenolic, lactone, and global primary groups) [21]. The iodine value (I_I) is a measure of the micropore content of a material. For this purpose, 0.05 g of AZO is placed in contact with 15 mL of I_2 solution (0.1 N). The mixture was stirred for 4–5 min, filtered, and dosed with a 0.1 N sodium thiosulphate solution. Starch was used as a color indicator [22].

The MB index represents the adsorption capacity of medium-sized molecules (mesopores and macropores) [23]. This method was used to determine the specific surface of the biomaterial (S_{MB}). It was calculated from the maximum amount of MB determined in the adsorption tests.

2.3. Instrument analysis

The morphology of AZO fine powder was visualized using scanning electron microscopy (SEM) (Quanta 650). The powder obtained from the AZO sawdust was characterized using FTIR spectroscopy, which was used to determine the functional groups of the AZO sawdust. The analysis is performed in the range of (400–4,000 cm^{-1}) on a

Bruker Alpha-T/P spectrometer. The AZO was also characterized by X-ray diffraction (XRD) using a Bruker D8 ADVANCE A25 Diffractometer to examine phases and crystallinity. Finally, the specific surface area was determined by the BET method using a Quantachrome 11.0 Instrument.

2.4. Adsorption experiments

To optimize the conditions for dye removal by the biomaterial, batch adsorption experiments were performed. A precise volume of the solution of known MB concentration is introduced into Erlenmeyer flasks containing a mass of AZO sawdust. The mixture thus prepared was placed on a mechanical shaker agitation at 200 revolutions/min (rpm), adjusting the desired pH and temperature values. Samples taken at regular times were filtered. The concentration of MB remaining in the supernatant solution was determined using an ultraviolet (UV)-visible spectrometer, at the wavelength corresponding to the maximum adsorption (664.5 nm). The adsorbed amount of MB per mass unit of the adsorbent at a time t, Q_{ads} (mg/g), and the removal percentage of the dye R (%) were calculated using Eqs. (2) and (3), respectively:

$$Q_{ads} = \frac{(C_0 - C_t) \times V}{m} \quad (2)$$

$$R(\%) = \frac{C_0 - C_t}{C_0} \times 100 \quad (3)$$

where C_0 (mg/L) is the initial concentration of MB, C_t (mg/L) is the dye concentration at time t, V (L) is the volume of the solution, and m (g) is the mass of the adsorbent.

To estimate the suitability of the kinetic and isothermal models used in this study, error analysis was evaluated by determining the correlation coefficient (R^2), the adjusted determination coefficient [R^2_{Adj}, Eq. (4)], the chi-square [χ^2, Eq. (5)] [24], and the normalized standard deviation [Δ (%), Eq. (6)] [25], using Origin Software (Version 18):

$$R^2_{Adj} = 1 - (1 - R^2)\left(\frac{n-1}{n-p}\right) \quad (4)$$

$$\chi^2 = \frac{\sum (Q_{e.exp} - Q_{e.th})}{Q_{e.th}} \quad (5)$$

$$\Delta(\%) = \sqrt{\frac{1}{n-1}\sum \left[\frac{Q_{e,exp} - Q_{e,cal}}{Q_{e,exp}}\right]^2} \times 100 \quad (6)$$

where n refers to the number of experimental data, p is the number of parameters of the fitted model, and $Q_{e,exp}$ (mg/g) and $Q_{e,th}$ (mg/g) are the experimental and calculated amounts of adsorbed dye at equilibrium, respectively.

3. Results and discussion

3.1. Chemical analysis

All surface chemical characteristics of AZO sawdust are shown in Table 1. The iodine value (I_I) and specific surface area (S_{MB}) suggested elevated porosity and good surface area of the raw AZO sawdust. Furthermore, the analysis of acidic and basic functional groups showed the acidic nature of the biomaterial surface with more carboxylic function (35.21%), thus favoring the adsorption of cationic dyes such as MB. pH_{PZC} (Fig. 1) was found to be equal to 6.28 (i.e., slightly acidic); so, at pH < 6.28, the surface of the sawdust was assumed to be positively charged, while at pH > 6.28 the surface was negatively charged. As the dye is cationic, it will be readily adsorbed in this pH range (i.e., pH > 6.28) [26,27].

3.2. SEM, FTIR, XRD and BET surface area analysis

In the SEM images obtained before and after adsorption (Fig. 2), cavities can be observed on the surface of the sawdust, indicating an irregular, porous, and strongly wavy structure. This structure is filamentary due to lignin and cellulose fibers, constituting large adsorption active sites and allowing the dye to be adsorbed. Moreover, it is clear that

Table 1
Chemical characteristics of Algerian Zean oak biosorbent

Parameters	
Acidic functions groups (mmol/g)	
Carboxylic	2.15
Lactonic	1.10
Phenolic	1.14
Total acidic	4.39
Total basic	1.52
Humidity content (%)	2.23
Ash content (%)	4.2
pH_{PZC}	6.28
I_I (mg/g)	342.63
S_{MB} (m^2/g)	128.21

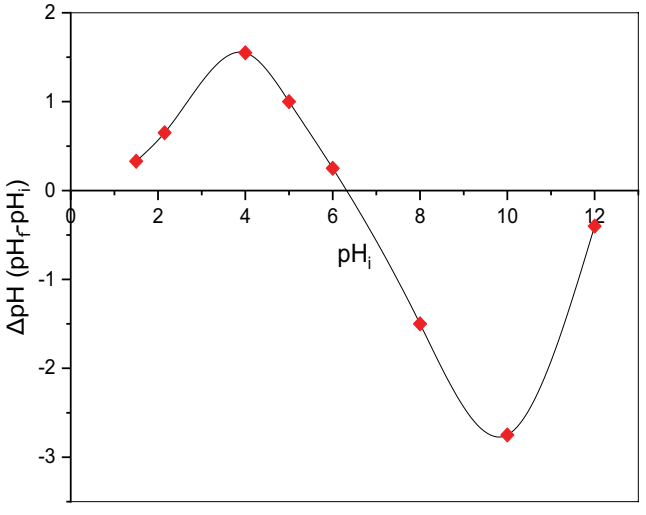

Fig. 1. Determination of the zero-charge point (pH_{PZC}) of Algerian Zean oak biosorbent.

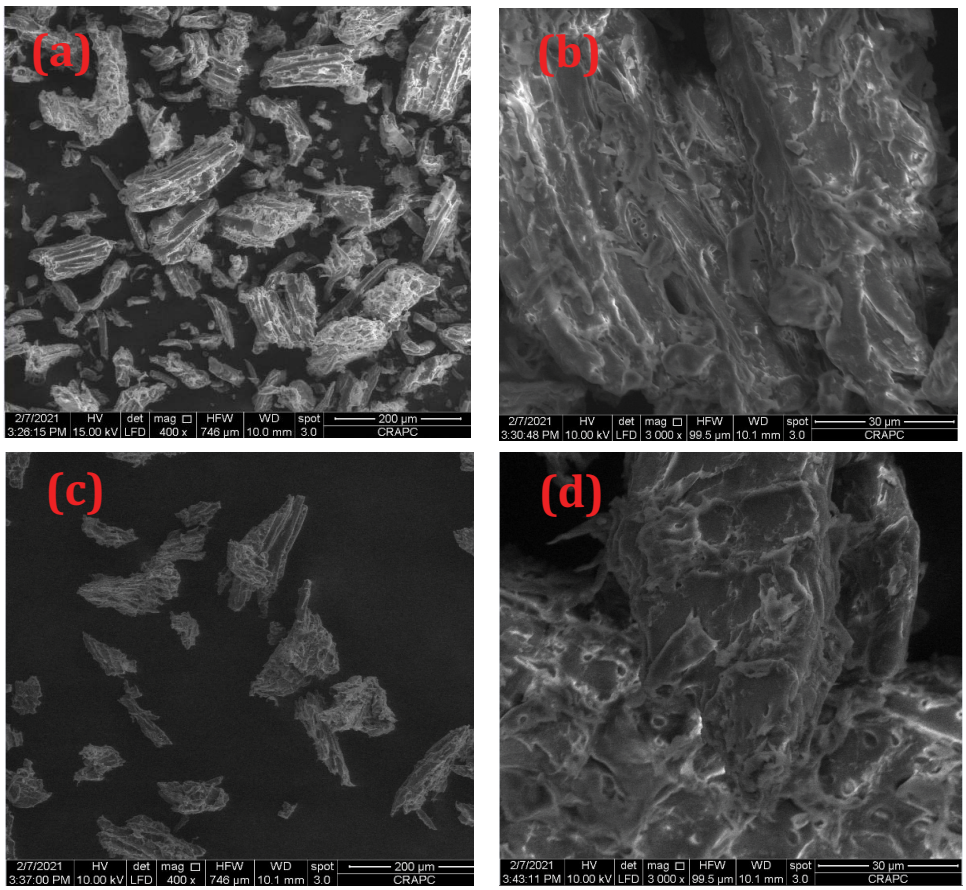

Fig. 2. Scanning electron micrograph of the Algerian Zean oak biosorbent: (a,b) before and (c,d) after methylene blue adsorption.

after adsorption, the surface of the adsorbent has undergone modifications, which implies that the adsorption has indeed taken place [28].

The FTIR spectra of AZO sawdust before and after adsorption (Fig. 3) showed several peaks, indicating that the biomaterial has several functional groups that form bonds with MB. The peak at 3,335 cm^{-1} is due to the stretching of the –OH group, mainly present in cellulose [29]. The band at 2,920 cm^{-1} corresponds to the stretching of the –CH bending band of the aliphatic groups (lignin, hemicellulose, and cellulose) [30], while the band around 1,730 cm^{-1} could be due to the C=O stretching of aldehydes, carboxylic, and esters or ketone in the lignin [19].

The peak at 1,595 cm^{-1} is attributed to the elongation vibration of the aromatic ring [31], while the attenuated band at 1,232 cm^{-1} may be due to the stretching of the phenolic group. The pronounced band at 1,025 cm^{-1} is attributed to the C–O and C–O–C groups of the ethers present in the cellulose [32]. The bands between 900 and 800 cm^{-1} are due to C–H vibrations. A faint peak at 897 cm^{-1} is observed, which is assigned to the vibrational nature of the glycosidic bonds owing to the presence of polysaccharides [33]. The broad bands that appear between 700 and 400 cm^{-1} are generally representative of the C–H group of cellulose [34]. After adsorption, the spectrum of the charged MB showed a broadly similar appearance to that of the crude sawdust. However, by looking closely at both spectra, shifts in some

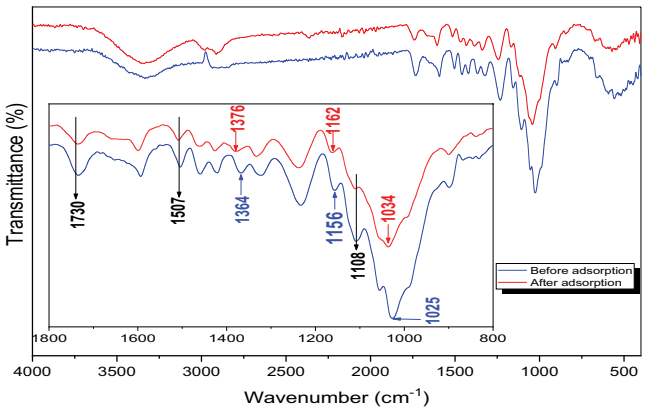

Fig. 3. Fourier-transform infrared spectra of Algerian Zean oak biosorbent before and after methylene blue adsorption.

peaks and changes in the intensity of others were noted. The peaks at 1,025 and 1,367 cm^{-1} are shifted to 1,034 and 1,379 cm^{-1}, indicating the contribution of the methoxy and C–H groups of alkanes to the MB removal, respectively. Moreover, the peaks at 1,108; 1,507 and 1,730 cm^{-1} altered in intensity, implicating the aromatic and carboxylic groups in the MB adsorption process. The slight shift of the peak from 1,156 to 1,162 cm^{-1} can be explained by the participation

of stretchable C–O of alcohols, esters, and carboxylic acids [35].

All the changes recorded in the spectrum of the dye-loaded sawdust suggest the implication of these functional groups in the adsorption process of the MB on the biomaterial [4].

The results of XRD analysis of AZO sawdust before and after adsorption of MB are shown in Fig. 4a. The diffractogram of the raw sawdust shows peaks characterizing the semi-crystalline structure of cellulose and hemicellulose at 2θ = 16°, 22.5° and 34.7° [36]. After treatment with MB, these peaks were shifted towards the higher 2θ, indicating the implication of the dye in the adsorption process [35].

To determine the specific surface area, pore volume, and pore size distribution of the AZO material, the BET method of nitrogen adsorption–desorption isotherms at 77 K was used. As shown in Fig. 4b and according to the IUPAC classification (International Union of Pure and Applied Chemistry), the adsorption–desorption isotherm of the raw sawdust is characterized by a combination of types I and II isotherms, revealing a variety of microporous and mesoporous structures [37]. The results show that AZO has a surface area equal to 10.17 m^2/g and an average pore size of 22.2 Å; this last value confirms the mesoporosity of the biomaterial [38].

3.3. Adsorption tests

The adsorption tests of MB on AZO sawdust were carried out by varying different experimental parameters.

3.3.1. Effect of contact time and particle size

Knowledge of the equilibrium time is necessary to establish the adsorption kinetics. Therefore, as a function of time, the adsorption tests were carried out in a discontinuous regime by putting in contact with 100 mL of MB solution at 20 mg/L with a mass of 0.1 g of AZO sawdust at different sizes (0.1, 0.5, and 1 mm).

The results (Fig. 5a) show that the MB adsorption efficiency increased rapidly in the first few minutes to 19.13, 17.61, and 15.47 mg/g, for sizes 0.1, 0.5, and 1 mm and for times of 45, 70, and 80 min, respectively. Then, it remained constant, indicating an equilibrium state. The adsorption equilibrium of the dye was very fast, and then it slowed down progressively.

This can be explained by the fact that initially, the adsorption sites of the sawdust were vacant and thus easily accessible to MB. However, the adsorption becomes less due to the slower diffusion of dissolved species through the pores of the adsorbent [39]. It is also noted that the adsorption efficiency was inversely proportional to the particle size. The finer the particle size, the more the specific surface area increases; consequently, the adsorption also increases [40]. Thus, the size of 0.1 mm is chosen for the rest of this study.

3.3.2. Effect of adsorbent dose

To evaluate the ideal amount of biosorbent to be added to the colored solution to remove MB, adsorption tests were performed by varying the mass of the adsorbent (from 0.1 to 4 g) using 100 mL of MB solution at 20 mg/g.

According to Fig. 5b, it was found that the percentage of MB removal depends significantly on the adsorbent mass removal percentage of MB removal as it increased proportionally with the mass of the adsorbent, going from 95% to 99.5% when the mass of the adsorbent increased from 0.1 to 5 g. But, then, it remained constant even when the amount of adsorbent was increased. This is due to the increase in the biomaterial surface area and the availability of high number of vacant active adsorption sites on this surface. Similar behavior was reported in MB removal onto palm bark and sugarcane bagasse [41]. In contrast,

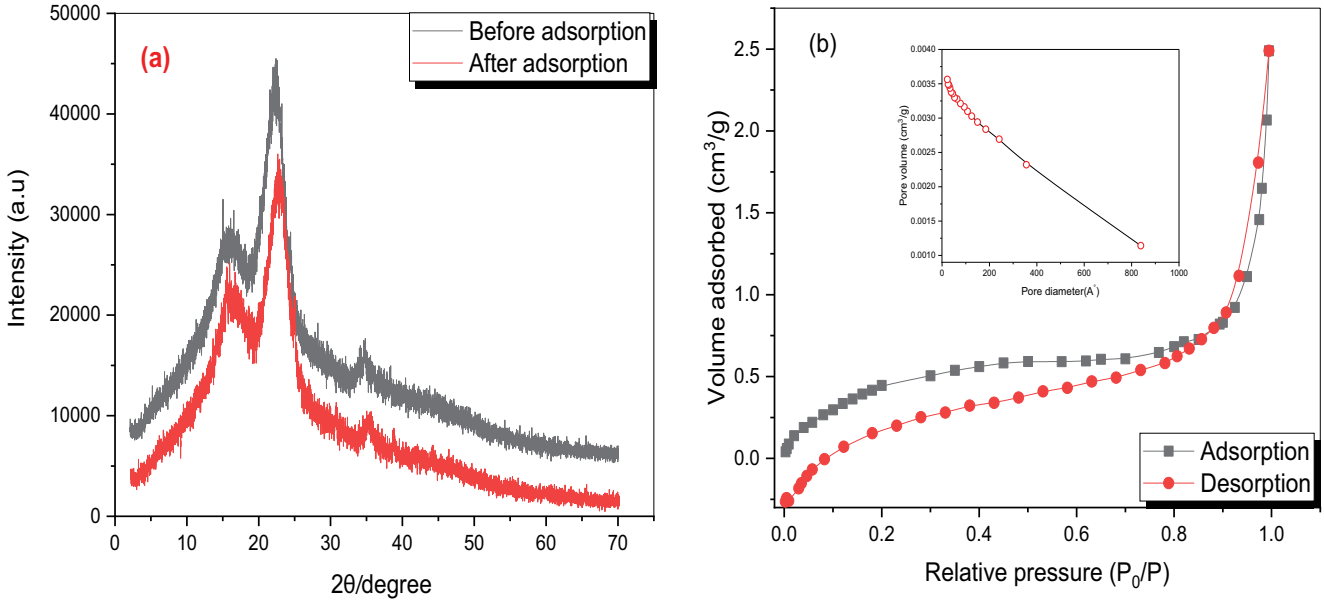

Fig. 4. (a) X-ray diffraction spectra and (b) N_2 adsorption–desorption isotherms of Algerian Zean oak biosorbent.

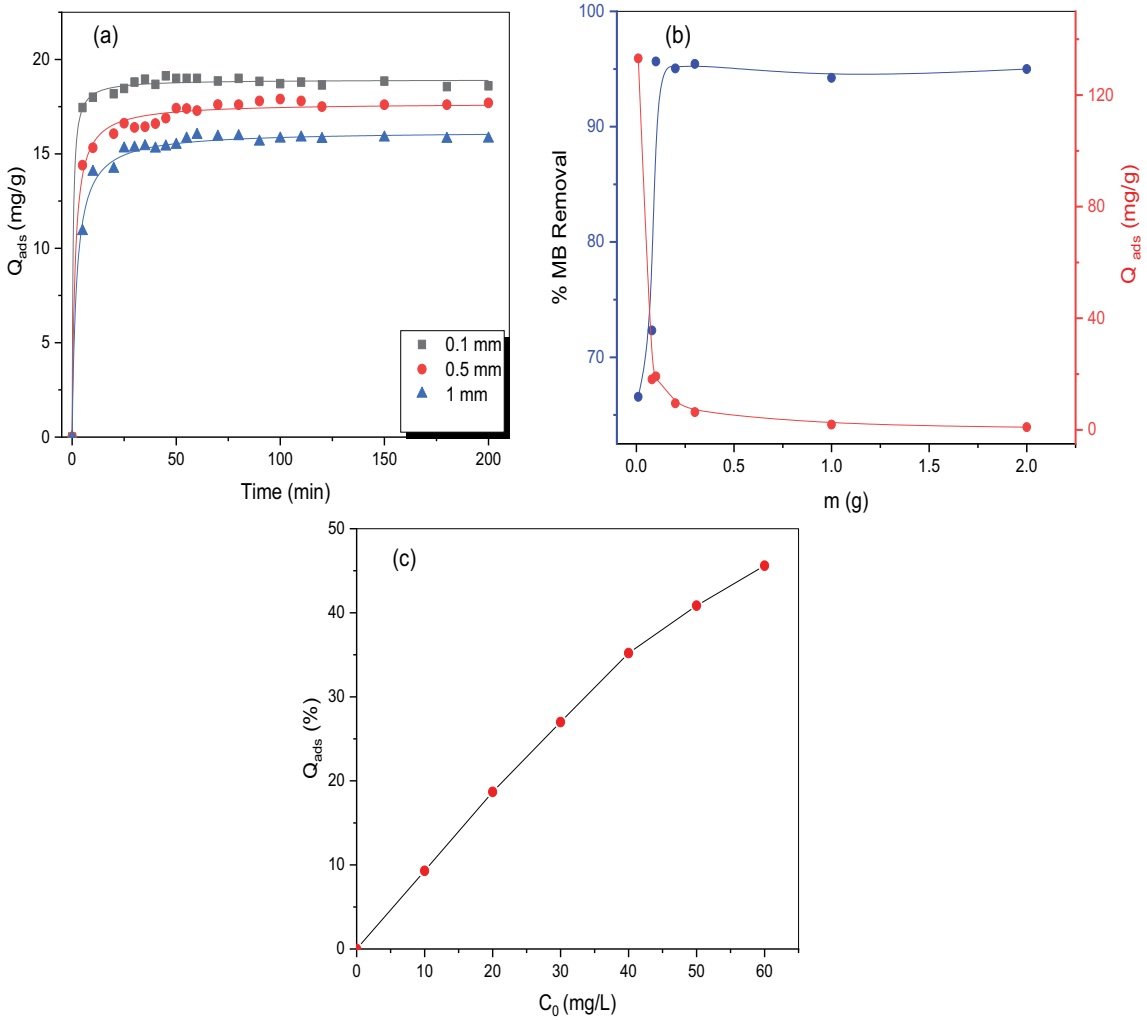

Fig. 5. Influence of: (a) contact time, (b) adsorbent mass and (c) initial methylene blue concentration on the adsorption of methylene blue on Algerian Zean oak biosorbent.

increasing the biosorbent dose decreased the absorbed amount, which could be explained by the non-saturation of the adsorption sites [42].

3.3.3. Effect of initial dye concentration

The initial dye concentration notably influences any adsorption study. Therefore, the process was performed to study the effects of MB concentration on adsorption capacity, with initial MB concentration ranging from 10 to 60 mg/L.

It can be observed that the amount of adsorbed dye increased with increasing the initial MB concentration (Fig. 5c).

After 100 min, the adsorbed amount increased from 18.69 to 45.6 mg/g when the initial concentration increased from 20 to 60 mg/g. This phenomenon can be explained by the fact that at high dye concentrations, the driving forces for mass transfer become sufficiently essential to overcome the mass transfer resistances of all adsorbent molecules between the aqueous and solid phases [24].

3.3.4. Effect of solution pH

The initial pH of the colored solutions is a very influential parameter in controlling the adsorption process. It directly impacts the quantity adsorbed as it can play on several parameters, such as the adsorbent surface charge, the adsorbate ionization degree, and the dissociation state of functional groups of the active adsorbent sites [33]. The pH effect was studied in the range of 1–11, using a 0.1 g mass of sawdust in 100 mL of 20 mg/L of MB solution.

The obtained results (Fig. 6a) showed that adsorption is low for acidic pH values (between 2 and 5), and then it increases to a pH of 7. Indeed, when an increase from 2 to 7 occurred in the pH, the capacity of MB adsorption increased significantly from 7.49 to 18.36 mg/g, respectively. The adsorbed amount of MB then slightly decreased for basic pH values. This leads to the conclusion that the adsorption of MB by the AZO biomaterial is favorable in a neutral medium. At low pH values, there is competition between excess H^+ ions and MB cations, which does not promote adsorption [43]. As the pH increases (from 5 to 7), the H^+ ions concentration decreases leading to good interaction between

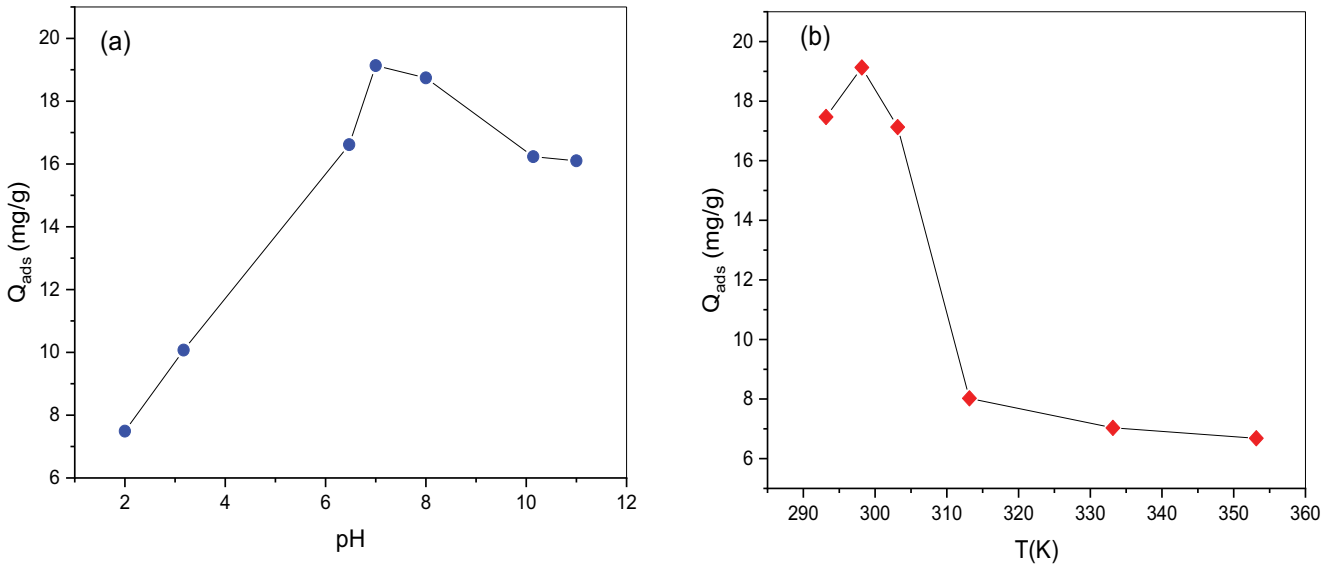

Fig. 6. Influence of: (a) pH and (b) temperature on the adsorption of methylene blue on Algerian Zean oak biosorbent.

the dye cations and the active sites on the adsorbent surface [44]. On the other hand, knowing that the biomaterial has a pH_{PZC} = 6.28 and the dye has a pK_a = 5.28 [45], the influence of pH on adsorption can be interpreted by the attraction between the negatively charged solid surface (pH < pH_{PZC}) and the positively charged cationic dye in a neutral medium (pH > pK_a), with a decrease in the concentration of H^+ protons in the solution, thus enhancing the adsorption of the MB. At pH < 6.28, the material's surface is protonated, adversely affecting the removal of the dye [46].

3.3.5. Effect of temperature

The temperature of the medium has a significant effect on the adsorption process. It is directly associated with the thermodynamic variables, enabling the determination of the adsorption nature. To determine its influence on the adsorption capacity, tests were carried out at optimal operating conditions (pH = 7, t = 60 min, C_0 = 20 mg/L), varying the temperature [from 298 K (25°C) to 353 K (80°C)] (Fig. 6b).

The obtained results show that the MB adsorbed amount decreased from 19.65 to 6.684 mg/g when the temperature increased from 298 to 353 K, revealing that the adsorption of MB is exothermic and is accompanied by a release of heat. This is the case with most adsorption processes, where high temperatures provoke displacement reverses of the adsorption equilibrium, thus facilitating desorption [47]. On the other hand, this can be explained by the weaker adsorption forces between the dye molecules and the active sites of the biosorbent [48]. Therefore, the effect of temperature was given as the last parameter. Moreover, 298 K is the most common working temperature.

3.4. Modeling adsorption kinetics

Adsorption kinetics describes the decrease in the adsorbate concentration in the solution as a function of the contact time with the adsorbent. It provides information about the adsorption mechanism and the mode of transfer of the solutes from the liquid to the solid phase. In this study, the adsorption kinetics is described by some commonly used models, namely the first and pseudo-second-order, Elovich, and intraparticle diffusion.

The linear form of the pseudo-first-order kinetic model is expressed by Eq. (7) [18]:

$$\mathrm{Ln}\left(Q_e - Q_t\right) = \mathrm{Ln}Q_e - \frac{K_1}{2.303}t \tag{7}$$

where Q_e (mg/g) and Q_t (mg/g) are the amounts of adsorbed dye at equilibrium and at a time t, respectively; t is time (min); K_1 (min^{-1}) is the pseudo-first-order adsorption rate constant.

Pseudo-second-order rate equation is given in the linearized form as [49]:

$$\frac{t}{Q_t} = \frac{1}{Q_e}t + \frac{1}{K_2 \cdot Q_e^2} \tag{8}$$

where K_2 (g/mg·min) is the adsorption constant of the pseudo-second-order, which is determined by drawing the graph $t/Q_t = f(t)$ (Fig. 7b).

Elovich model is represented by Eq. (9) [50]:

$$Q_t = \frac{1}{\beta}\mathrm{Ln}\left(\alpha\beta\right) + \frac{1}{\beta}\mathrm{Ln}t \tag{9}$$

where a (mg/g·min) is the initial adsorption rate, while b (g/mg) is the desorption constant.

To identify the diffusion mechanism, the kinetic results were then examined using the intraparticle diffusion model. According to Weber and Morris [51], the kinetic expression for intraparticle diffusion is often presented by:

$$Q_t = K_i\sqrt{t} + C \tag{10}$$

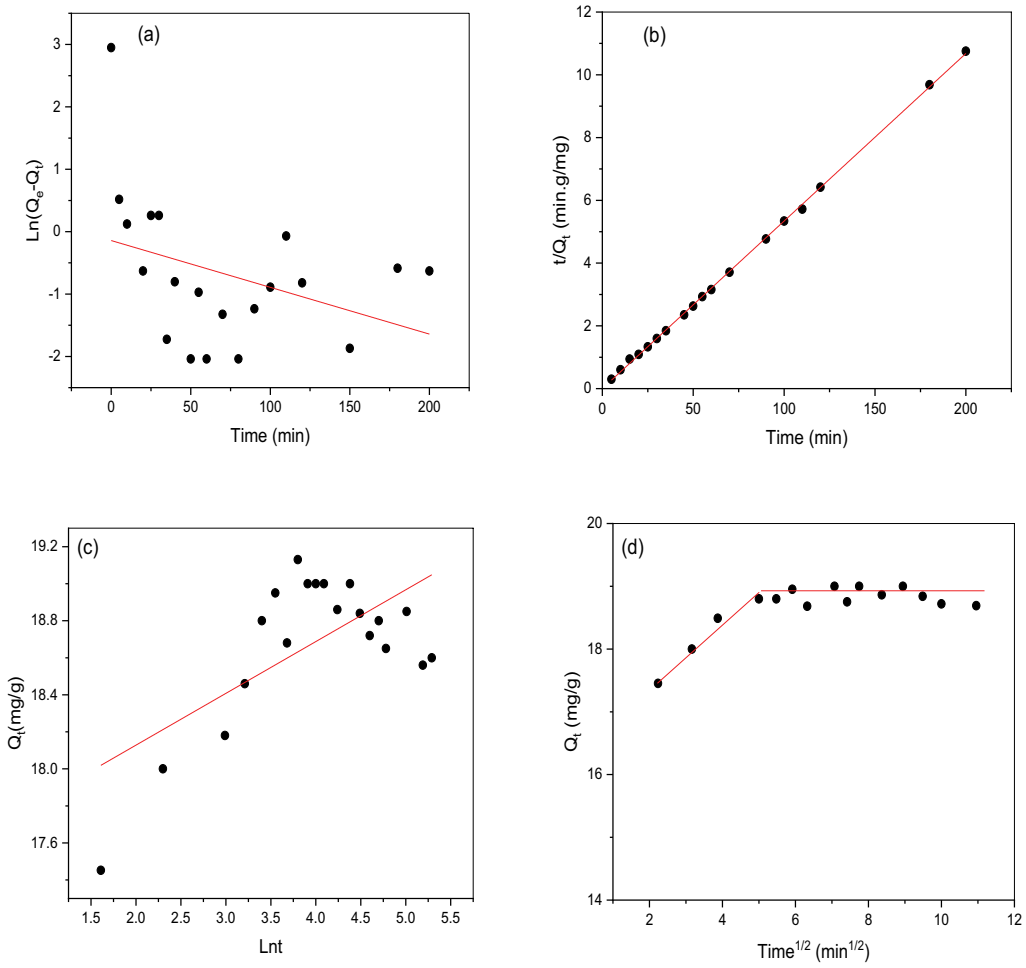

Fig. 7. Kinetic models applied to methylene blue adsorption on Algerian Zean oak biosorbent: (a) pseudo-first-order, (b) pseudo-second-order, (c) Elovich, and (d) intraparticle diffusion.

where K_i is the intraparticle diffusion rate constant. The value of the intercept C (mg/g) indicates the boundary layer thickness.

The different kinetic parameters for MB adsorption onto the AZO are regrouped in Table 2.

For the pseudo-first-order model, it is noted that the adsorbed amount is very low compared to the experimental one (Table 2). Estimating the different error parameters (R^2, R^2_{Adj}, and Δ (%)) predicts that the pseudo-first-order model does not correspond well to the experimental results. In parallel, the adsorbed quantity calculated by the pseudo-second-order (Fig. 7b) is closer to that determined by the experiments, which is proved by the high value of the correlation coefficient R^2 (0.999) and the value of R^2_{Adj} (0.999) and the lower normalized standard deviation Δ (%).

All these observations suggest the feasibility of the pseudo-second-order model on MB adsorption in this study. On the other hand, the low values of R^2 (0.428), R^2_{Adj} (0.396), and the inflated value of Δ (%) indicated the non-applicability of the Elovich model to the adsorption of MB on AZO (Table 2).

For the intraparticle model, the intercept did not pass through the origin (Fig. 7d), indicating that intraparticle diffusion was not the rate-controlling step. Thus, it can be concluded that intraparticle diffusion is not the determining mechanism of MB adsorption on the AZO adsorbent; it exists but occurs together with different diffusion mechanisms. The presence of two distinct regions is revealed. The first stage involves the diffusion of molecules into the solid. Generally, this is the longest stage. The second stage represents adsorption, where the reaction occurs. Moreover, the rate constant K_1 of the first step was higher than that of the second, and MB was adsorbed rapidly by the external surface. Once this surface was saturated, the dye molecules diffused into the pores of the inner surface, where the diffusion resistance increased, reducing the diffusion rate [52].

3.5. Adsorption isotherm

The parameters obtained from isotherm modeling provide essential information on the adsorption mechanism, surface properties, and adsorbent–adsorbate affinities [53]. Among the most commonly used models are the Langmuir, Freundlich, Sips, and Redlich–Peterson models.

Langmuir isotherm model is widely used. It describes most adsorption reactions. This model assumes that the

Table 2
Kinetic parameters for methylene blue adsorption onto Algerian Zean oak biosorbent

Kinetic model	Parameters	
	C_0 (mg/L)	20
	$Q_{e,exp}$ (mg/g)	19.13
	$Q_{e,th}$ (mg/g)	0.868
Pseudo-first-order	K_1 (min^{-1})	0.017
	R^2	0.133
	R^2_{Adj}	0.085
	Δ (%)	>50
	$Q_{e,th}$ (mg/g)	18.72
	K_2 (g/mg·min)	5.7
Pseudo-second-order	R^2	0.999
	R^2_{Adj}	0.999
	Δ (%)	2.53
	b (g/mg)	0.0035
	a (mg/g·min)	1.065
Elovich	R^2	0.428
	R^2_{Adj}	0.396
	Δ (%)	>50
	K_{i1} (mg/g·min$^{1/2}$)	0.496
	C_1	16.416
	R_1^2	0.963
	$R^2_{Adj,1}$	0.945
Intraparticle diffusion	K_{i2} (mg/g·min$^{1/2}$)	0.033
	C_2	19.081
	R_2^2	0.882
	$R^2_{Adj,2}$	0.873
	Δ (%)	2.3

adsorbed species is fixed on a single well-defined site, each site is only able to fix one adsorbed species, the adsorption is a monolayer, the surface is homogeneous and there is no interaction between the adsorbed molecules [18,54]. The Langmuir isotherm is given as:

$$Q_e = \frac{Q_m K_L C_e}{1 + K_L C_e} \tag{11}$$

where C_e (mg/L) is the equilibrium concentration of the adsorbate, while Q_m (mg/g) is the maximum adsorbed amount and K_L (L/mg) is the Langmuir constant related to the adsorption energy. A plot of C_e/Q_e vs. C_e (Fig. 7a) allows calculating the parameters Q_m and K_L from the intercept and the slope, respectively. An essential characteristic of the Langmuir isotherm can be expressed in terms of a dimensionless constant R_L called separation factor. It is defined by Eq. (12) [55]:

$$R_L = \frac{1}{1 + k_L C_0} \tag{12}$$

where C_0 is the initial concentration of MB (mg/L) and R_L values indicate if the adsorption is unfavorable ($R_L > 1$), linear ($R_L = 1$), favorable ($0 < R_L < 1$) or irreversible ($R_L = 0$).

Freundlich model represents non-ideal adsorption on heterogeneous surfaces as well as multilayer adsorption. Its empirical formula is given by Eq. (13) [56]:

$$Q_e = K_F C_e^{\frac{1}{n}} \tag{13}$$

where K_F and n are Freundlich constants. K_F is an indication of the adsorption capacity of the material, n represents the adsorption intensity and indicates whether adsorption is feasible. If $n = 1$, adsorption is linear; if $n < 1$, adsorption is chemical; and if $n > 1$, adsorption is then physical and favorable [55].

Redlich–Peterson (R-P) model is applied considering the limits of both Langmuir and Freundlich models [57]. It incorporates the characteristics of the isotherms of both models in a single mathematical equation, which is applied in homogeneous and heterogeneous systems due to its versatility. The R-P model equation is expressed as:

$$Q_e = \frac{K_{R-P} C_e}{1 + C_e^a} \tag{14}$$

where $K_{R\text{-}P}$, b, and a are the Redlich–Peterson constants, a must be in the range [0–1]; if $a = 1$, the isotherm is Langmuir; if $a = 0$, the isotherm is then Freundlich [58].

Sips model is an equation based on Langmuir and Freundlich isotherms at the same time [57]. It describes heterogeneous surfaces well. The equation can be written as:

$$Q_e = Q_m \frac{K_S C_e^n}{1 + K_S C_e^n} \tag{15}$$

where K_S (L/mg) is the Langmuir–Freundlich constant related to the energy of the adsorption.

Temkin isotherm model contains a factor that explicitly takes adsorbate–adsorbent species interactions into account. It also assumes that the adsorption heat of all molecules decreases linearly with the coverage involved in this interaction [58]. The Temkin model equation is expressed as follows:

$$Q_e = B \ln K_T C_e \tag{16}$$

$$B = \frac{RT}{b_T} \tag{17}$$

where K_T (L/mg) and b_T (J/mol) are the Temkin constants; K_T corresponds to the maximum binding energy, while the constant B is related to the adsorption heat.

The isotherm parameters calculated for the adsorption of MB by AZO sawdust are summarized in Table 3. These results show that the experimental data are very coherent with the Langmuir model (Fig. 8a). This hypothesis is confirmed by the high values of the correlation coefficients R^2 (0.985), adjusted determination coefficients R^2_{Adj} (0.982) and lower values of chi-square χ^2 (4.121) and Δ (%) (3.9). Moreover, a maximum adsorbed quantity of 52.376 mg/g is obtained, which is very close to the experimental value of 51.75 mg/g. The separation factor R_L, which could indicate

Table 3
Isotherm parameters for methylene blue adsorption onto Algerian Zean oak biosorbent

Isotherm model	Parameters	
Langmuir	Q_{esp} (mg/g)	51.750
	Q_{max} (mg/g)	52.376
	K_L (L/mg)	0.487
	R_L	0.093 (C_0 = 20 mg/L)
	R^2	0.985
	R^2_{Adj}	0.982
	χ^2	4.121
	Δ (%)	3.9
Freundlich	K_F	20.651
	n	3.787
	R^2	0.901
	R^2_{Adj}	0.887
	χ^2	27.113
	Δ (%)	28.83
Redlich–Peterson (R-P)	K_{R-P}	30.408
	b	0.695
	a	0.946
	R^2	0.988
	R^2_{Adj}	0.984
	χ^2	3.707
	Δ (%)	5
Sips	Q_m	55.826
	K_S	0.470
	n	0.839
	R^2	0.989
	R^2_{Adj}	0.986
	χ^2	3.25
	Δ (%)	2.9
Temkin	K_T (L/g)	7.768
	b_T (kJ/mol)	0.266
	R^2	0.973
	R^2_{Adj}	0.969
	χ^2	7.768
	Δ (%)	6.9

adsorbent-dye affinity showed favorable dye adsorption [0.093–0.033] for all initial concentrations of MB (20–60 mg/L), respectively. The applicability of this model (i.e., Langmuir) revealed the chemical nature of the adsorption, which is mainly monolayer. The surface of the AZO adsorbent is energetically homogeneous with monomolecular adsorption. The R^2, R^2_{Adj}, χ^2, and Δ (%) obtained with the Freundlich model (Table 3) suggested that this model is not suitable for the adsorption of MB on AZO biomaterial. However, the higher value of n (3.787) could well mean that the biosorption of MB on the surface of AZO is favorable. The MB adsorption isotherm experimental data were also fitted using the Redlich–Peterson model (Fig. 8a). Regarding the compatibility of the results, the rather high values of R^2, R^2_{Adj} and the low value of χ^2 (Table 3) gave a very satisfactory result.

Further, the value of n (0.946) is very close to 1 confirming that the Langmuir model described better the MB adsorption isotherm than the Freundlich model [59]. Isotherm modeling of the two models Sips and Temkin is shown in Fig. 7b. The Sips model seems to fit the adsorption isotherm well, with a good correlation coefficient (R^2 = 0.989) and low values of χ^2 and Δ (%). Moreover, the maximum value of the calculated adsorbed quantity, which is very close to the experimental value (Table 3), also suggests that this model clearly describes the data obtained in this study, compared to Temkin's model in which all the results acquired to confirm the lack of agreement of this model with the adsorption of MB by AZO.

By comparing the maximum MB amount adsorbed by AZO sawdust with other materials (Table 4), the results highlighted that this biosorbent achieved a very satisfying adsorption performance.

3.6. Thermodynamic studies

The analysis of the thermodynamic parameters is necessary for predicting the phenomenon of adsorption. Gibbs free energy ΔG° (kJ/mol), enthalpy ΔH° (kJ/mol), and entropy ΔS° (kJ/mol·K) are determined using Eqs. (18)–(20):

$$K_c = \frac{Q_e}{C_e} \tag{18}$$

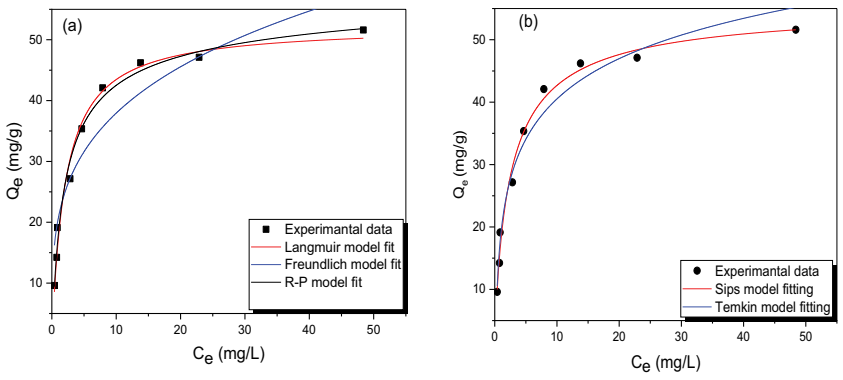

Fig. 8. Isotherm models applied to methylene blue adsorption on Algerian Zean oak biosorbent: (a) Langmuir, Freundlich and Redlich–Peterson and (b) Sips and Temkin.

$$\ln K_c = -\frac{\Delta H^\circ}{RT} + \frac{\Delta S^\circ}{R} \quad (19)$$

$$\Delta G^\circ = -RT \ln K_c \quad (20)$$

where: K_c (L/g) is the equilibrium constant at different temperatures. ΔH° and ΔS° are determined from the slope and intercept of the plot of $\ln K_c$ vs. $(1/T)$ using the van't Hoff plot (Fig. 9). The different thermodynamic parameters are gathered in Table 5.

The adsorption of MB onto AZO sawdust is exothermic, confirmed by the negative value of ΔH (Table 5). The negatively decreasing of ΔG with increases in temperature from 298 to 353 K revealed the spontaneity of the adsorption process. The negative entropy value indicated the increase in the randomness of the solid–liquid interface [65], reflecting the low affinity of the biosorbent for the dye during the adsorption process. Similar results have also been reported by Fayoud et al. [61].

4. Proposed adsorption mechanism

According to the results illustrated in this study, the primary mechanisms responsible for the adsorption of MB dye molecules on the AZO biomaterial have been highlighted. Indeed, the data suggest that physical forces and chemical interactions may be involved in these mechanisms (Fig. 10). FTIR analysis (Fig. 3) and chemical characteristics of the AZO surface (Table 1) showed a structure rich in oxygenated groups (carboxylic and hydroxyl) that may interact via hydrogen bonds (also known as dipole–dipole bonds) with MB molecules [66]. In this case, as hydrogen donors, the hydroxyl groups of the adsorbent will interact with the nitrogen and oxygen (H-acceptor) to create these interactions. These mechanisms may also involve physical interactions other than hydrogen bonding involving the carboxyl group. They include electrostatic interactions between the negative sites of the carboxyl functional groups and the

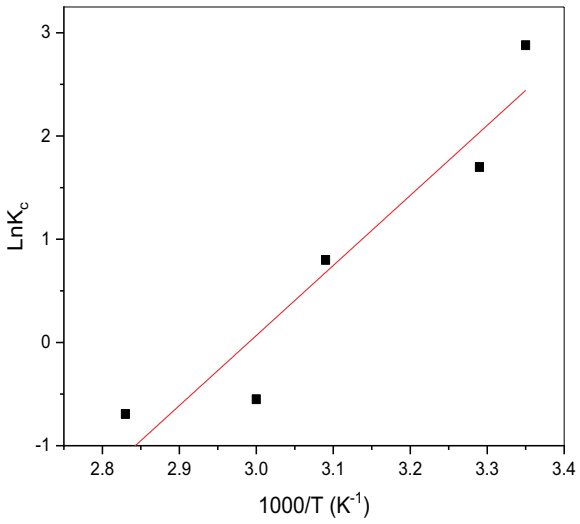

Fig. 9. van't Hoff curve for methylene blue adsorption on Algerian Zean oak biosorbent.

Table 4
Comparison of methylene blue capacity onto various adsorbents materials comprising Algerian Zean oak sawdust that is investigated in this work

Adsorbents	Q_{max} (mg/g)	References
Orange and banana peels	13.9	[60]
Wood ash	50	[61]
Pyrophyllite	4.2	[62]
Eucalyptus grandis sawdust	32	[63]
Pomegranate peel activated carbon	5.03	[24]
Ginkgo biloba leaves	48.07	[39]
Ultrasonic modified chitin	26.7	[64]
Carboxyl-functionalized magnetic nanoparticle	43.15	[45]
Eucalyptus globulus sawdust	6.6	[7]
Fungal biomass	16.67	[46]
AZO sawdust	52.376	This work

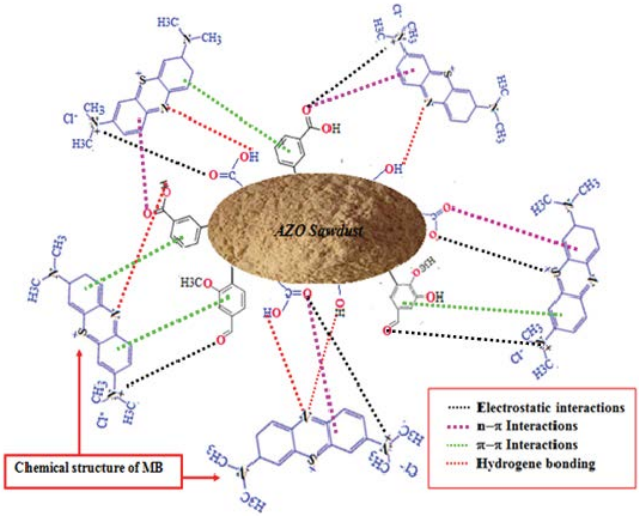

Fig. 10. Possible interactions between Algerian Zean oak sawdust and methylene blue molecules.

Table 5
Thermodynamic parameters for methylene blue adsorption onto Algerian Zean oak biosorbent

ΔH (kJ/mol)	ΔS (kJ/mol·K)	ΔG (kJ/mol)				
		298.15 K	303.15 K	313.15 K	333.15 K	353.15 K
–56.41	–0.168	–106.5	–107.34	–109.02	–112.38	–115.75

cationic N^+ and S^+ groups of the MB [63,67]. Further, n–π interactions between the (–COO^-–) groups of the sawdust as n-donors and the n-acceptor sites of the aromatic ring of the MB could also occur. On the other hand, aromatic rings' impact on the chemical structure of sawdust and MB dye may also promote π–π interactions [12,29,51].

5. Conclusion

The present study successfully evaluated Algerian Zean oak (AZO) sawdust to prepare a new, natural, available, and inexpensive adsorbent for removing methylene blue (MB). After the characterization of the biomaterial with several techniques, the morphology of AZO by SEM indicated a structure consisting of large active sites offering a great possibility of dye adsorption. FTIR analysis revealed the involvement of several functional groups in the adsorption process, such as carboxyl and hydroxyl groups. Experiments in the batch mode were carried out to obtain the optimum adsorption parameters of the MB. The kinetic study showed that adsorption is rapid; equilibrium is reached after 45 min. AZO powder with a porosity of 0.1 mm was the most effective in removing methylene blue dye from aqueous solutions. The optimal biomaterial dose for MB biosorption is 1 g/L, and the best degradation occurred at neutral pH, room temperature, and 20 mg/L dye concentration. The pseudo-second-order kinetic model well described the adsorption mechanism. The adsorption isotherms of MB on the biomaterial are in good agreement with the Sips model, followed by Langmuir, confirming a chemical and monolayer adsorption on the homogeneous surface of the adsorbent. The negative value of Gibbs free energy changes (–106.5 kJ/mol) indicates the spontaneous nature of the adsorption, while the negative value of enthalpy suggests an exothermic process (–56.41 kJ/mol). Moreover, the negative entropy value indicated the increase in the randomness of the solid–liquid interface (–0.168 kJ/mol·K). At the end of this study, it is concluded that AZO sawdust will make an alternative, natural, available, and inexpensive means for the adsorption and removal of MB from aqueous solutions.

Acknowledgements

The authors would like to thank the Ministry of Higher Education and Scientific Research (MESRS), Algeria, for supporting the present research.

The Center for Scientific and Technical Research in Physical and Chemical Analysis (CRAPC) is sincerely thanked for the FTIR and SEM analyses.

References

[1] T. Ainane, F. Khammour, M. Talbi, M. Elkouali, A novel bio-adsorbent of mint waste for dyes remediation in aqueous environments: study and modeling of isotherms for removal of methylene blue, Orient. J. Chem., 30 (2014) 1183–1189.
[2] G.A.A. Al-Hazmi, M.A. El-Bindary, M.G. El-Desouky, A.A. El-Bindary, Efficient adsorptive removal of industrial dye from aqueous solution by synthesized zeolitic imidazolate framework-8 loaded date seed activated carbon and statistical physics modeling, Desal. Water Treat., 258 (2022) 85–103.
[3] N. El Messaoudi, M. El Khomri, A. El Mouden, A. Bouich, A. Jada, A. Lacherai, H.M.N. Iqbal, S.I. Mulla, V. Kumar, J.H.P. Américo-Pinheiro, Regeneration and reusability of non-conventional low-cost adsorbents to remove dyes from wastewaters in multiple consecutive adsorption–desorption cycles: a review, Biomass Convers. Biorefin., (2022), doi: 10.1007/s13399-022-03604-9.
[4] S. Banerjee, M.C. Chattopadhyaya, Adsorption characteristics for the removal of a toxic dye, tartrazine from aqueous solutions by a low cost agricultural by-product, Arabian J. Chem., 10 (2017) S1629–S1638.
[5] A.S. ALzaydien, Adsorption of methylene blue from aqueous solution onto a low-cost natural jordanian tripoli, Am. J. Environ. Sci., 5 (2009) 197–208.
[6] N.B. Prakash, V. Sockan, P. Jayakaran, Waste water treatment by coagulation and flocculation, Int. J. Eng. Sci. Innov. Technol., 3 (2014) 479–484.
[7] H. Akrout, S. Jellali, L. Bousselmi, Enhancement of methylene blue removal by anodic oxidation using BDD electrode combined with adsorption onto sawdust, C.R. Chim., 18 (2015) 110–120.
[8] Z. Isik, E.B. Arikan, H.D. Bouras, N. Dizge, Bioactive ultrafiltration membrane manufactured from *Aspergillus carbonarius* M333 filamentous fungi for treatment of real textile wastewater, Bioresour. Technol. Rep., 5 (2019) 212–219.
[9] O. Baaloudj, I. Assadi, N. Nasrallah, A. El Jery, L. Khezami, A.A. Assadi, Simultaneous removal of antibiotics and inactivation of antibiotic-resistant bacteria by photocatalysis: a review, J. Water Process Eng., 42 (2021) 102089, doi: 10.1016/j.jwpe.2021.102089.
[10] R. Javaid, U.Y. Qazi, Catalytic oxidation process for the degradation of synthetic dyes: an overview, Int. J. Environ. Res. Public Health, 16 (2019) 1–27.
[11] Y. Lu, L.B.L. Lim, N. Priyantha, Chemical modification of pomelo leaves as a simple and effective way to enhance adsorption toward methyl violet dye, Desal. Water Treat., 197 (2020) 379–391.
[12] N. El Messaoudi, M. El Khomri, Z. Goodarzvand Chegini, N. Chlif, A. Dbik, S. Bentahar, M. Iqbal, A. Jada, A. Lacherai, Desorption study and reusability of raw and H_2SO_4 modified jujube shells (*Zizyphus lotus*) for the methylene blue adsorption, Int. J. Environ. Anal. Chem., (2021) 1–17, doi: 10.1080/03067319.2021.1912338.
[13] S.A. Prabhakar, N. Ojha, N. Das, Application of *Aloe vera* mucilage as bioflocculant for the treatment of textile wastewater: process optimization, Water Sci. Technol., 82 (2020) 2446–2459.
[14] G.K. Cheruiyot, W.C. Wanyonyi, J.J. Kiplimo, E.N. Maina, Adsorption of toxic crystal violet dye using coffee husks: equilibrium, kinetics and thermodynamics study, Sci. Afr., 5 (2019) 1–11.
[15] M. El Khomri, N. El Messaoudi, A. Dbik, S. Bentahar, A. Lacherai, N. Faska, A. Jada, Regeneration of argan nutshell and almond shell using HNO_3 for their reusability to remove cationic dye from aqueous solution, Chem. Eng. Commun., 209 (2022) 1304–1315.
[16] S.N.A.S. Ismail, W.A. Rahman, N.A.A. Rahim, N.D. Masdar, M.L. Kamal, Adsorption of malachite green dye from aqueous solution using corn cob, AIP Conf. Proc., 2031 (2018), doi: 10.1063/1.5066992.
[17] S. Arya, D. Studies, Removal of hexavalent chromium from aqueous solutions using sawdust as a low cost adsorbent, Int. J. Adv. Res. Sci. Technol., 3 (2015) 99–105.
[18] D.C.C. Da Silva, J.M.T.D.A. Pietrobelli, Residual biomass of chia seeds (*Salvia hispanica*) oil extraction as low cost and eco-friendly biosorbent for effective reactive yellow B2R textile dye removal: characterization, kinetic, thermodynamic and isotherm studies, J. Environ. Chem. Eng., 7 (2019) 103008, doi: 10.1016/j.jece.2019.103008.
[19] Y. Djilali, E.H. Elandaloussi, A. Aziz, L.C. de Ménorval, Alkaline treatment of timber sawdust: a straightforward route toward effective low-cost adsorbent for the enhanced removal of basic dyes from aqueous solutions, J. Saudi Chem. Soc., 20 (2016) S241–S249.
[20] D. Badis, Z. Benmaamar, O. Benkortbi, H. Boutoumi, H. Hamitouche, A. Aggoun, Removal of methylene blue by

adsorption onto retama raetam plant: kinetics and equilibrium study, Chem. J. Mold., 11 (2016) 74–83.
[21] G. Özsin, M. Kılıç, E. Apaydın-Varol, A.E. Pütün, Chemically activated carbon production from agricultural waste of chickpea and its application for heavy metal adsorption: equilibrium, kinetic, and thermodynamic studies, Appl. Water Sci., 9 (2019), doi: 10.1007/s13201-019-0942-8.
[22] E.K. Doboy, H.Z. Adjia, R. Kamga, Production and characterization of rice husk biosorbent from Far North Cameroon, Environ. Pollut., 8 (2019) 1, doi: 10.5539/ep.v8n2p1.
[23] K.M. Kifuani, A. Kifuani Kia Mayeko, B. Ilinga Lopaka, P. Ngoy Bokolombe, T. Monama Ondongo, G. Ekoko Bakambo, J. Muswema Lunguya, Kinetic and thermodynamic studies adsorption of methylene blue (MB) in aqueous solution on a bioadsorbent from *Cucumeropsis mannii* Naudin waste seeds, Int. J. Biol. Chem. Sci., 12 (2019) 2412, doi: 10.4314/ijbcs.v12i5.38.
[24] I.Y. Erwa, O.A. Ishag, O.A. Alrefaei, I.M. Hassan, Nonlinear fitting for estimation of adsorption equilibrium, kinetic and thermodynamic parameters of methylene blue onto activated carbon, J. Turk. Chem. Soc. Sect. A Chem., 9 (2022) 67–84.
[25] B. Belhamdi, Z. Merzougui, M. Trari, A. Addoun, A kinetic, equilibrium and thermodynamic study of L-phenylalanine adsorption using activated carbon based on agricultural waste (date stones), J. Appl. Res. Technol., 14 (2016) 354–366.
[26] H.A. Al-Aoh, M.M.H. Aljohani, A.A.A. Darwish, M. Ayaz Ahmad, S.A. Bani-Atta, M.A. Alsharif, Y.M. Mahrous, S.K. Mustafa, H.S. Al-Shehri, L.R. Alrawashdeh, J.N. Al-Tweher, A potentially low-cost adsorbent for methylene blue removal from synthetic wastewater, Desal. Water Treat., 213 (2021) 431–440.
[27] A. El Mouden, N. El Messaoudi, A. El Guerraf, A. Bouich, V. Mehmeti, A. Lacherai, A. Jada, F. Sher, Multifunctional cobalt oxide nanocomposites for efficient removal of heavy metals from aqueous solutions, Chemosphere, 317 (2023) 137922, doi: 10.1016/j.chemosphere.2023.137922.
[28] M.N. Ashiq, M. Najam-Ul-Haq, T. Amanat, A. Saba, A.M. Qureshi, M. Nadeem, Removal of methylene blue from aqueous solution using acid/base treated rice husk as an adsorbent, Desal. Water Treat., 49 (2012) 376–383.
[29] M. Àngels Olivella, N. Fiol, F. de la Torre, J. Poch, I. Villaescusa, A mechanistic approach to methylene blue sorption on two vegetable wastes: cork bark and grape stalks, BioResources, 7 (2012) 3340–3354.
[30] F. Deniz, R.A. Kepekci, Bioremoval of malachite green from water sample by forestry waste mixture as potential biosorbent, Microchem. J., 132 (2017) 172–178.
[31] J.J. Salazar-Rabago, R. Leyva-Ramos, J. Rivera-Utrilla, R. Ocampo-Perez, F.J. Cerino-Cordova, Biosorption mechanism of methylene blue from aqueous solution onto white pine (*Pinus durangensis*) sawdust: effect of operating conditions, Sustain. Environ. Res., 27 (2017) 32–40.
[32] A. Ismaili M'hamdi, N. Idrissi Kandri, A. Zerouale, Adsorption study of the methylene blue on sawdust beech and red wood, J. Mater. Environ. Sci., 8 (2017) 2816–2831.
[33] H. Grabi, F. Derridj, W. Lemlikchi, E. Guénin, Studies of the potential of a native natural biosorbent for the elimination of an anionic textile dye cibacron blue in aqueous solution, Sci. Rep., 11 (2021) 1–13.
[34] D. Prabu, P.S. Kumar, K.H. Vardhan, S. Sathish, A. Raju, J. Mathew, Adsorptive elimination of methylene blue dye from aquatic system using biochar produced from cocoa shell, Desal. Water Treat., 203 (2020) 366–378.
[35] H.B. Motejadded Emrooz, M. Maleki, A. Rashidi, M. Shokouhimehr, Adsorption mechanism of a cationic dye on a biomass-derived micro- and mesoporous carbon: structural, kinetic, and equilibrium insight, Biomass Convers. Biorefin., 11 (2021) 943–954.
[36] N. Nordine, Z. El Bahri, H. Sehil, R.I. Fertout, Z. Rais, Z. Bengharez, Lead removal kinetics from synthetic effluents using Algerian pine, beech and fir sawdust's: optimization and adsorption mechanism, Appl. Water Sci., 6 (2016) 349–358.
[37] J.-X. Yang, G.-B. Hong, Adsorption behavior of modified *Glossogyne tenuifolia* leaves as a potential biosorbent for the removal of dyes, J. Mol. Liq., 252 (2018) 289–295.
[38] W.S. Wan Ngah, M.A.K.M. Hanafiah, S.S. Yong, Adsorption of humic acid from aqueous solutions on crosslinked chitosan-epichlorohydrin beads: kinetics and isotherm studies, Colloids Surf., B, 65 (2008) 18–24.
[39] R. Singh, T.S. Singh, J.O. Odiyo, J.A. Smith, J.N. Edokpayi, Evaluation of methylene blue sorption onto low-cost biosorbents: equilibrium, kinetics, and thermodynamics, J. Chem., 2020 (2020), doi: 10.1155/2020/8318049.
[40] N. Barka, K. Ouzaouit, M. Abdennouri, M. El Makhfouk, Dried prickly pear cactus (*Opuntia ficus indica*) cladodes as a low-cost and eco-friendly biosorbent for dyes removal from aqueous solutions, J. Taiwan Inst. Chem. Eng., 44 (2013) 52–60.
[41] A. Aarfane, S. Tahiri, A. Salhi, G. El Kadiri Boutchich, M. Siniti, M. Bensitel, B. Sabour, M. El Krati, Adsorption of methylene blue and red 195 dyes in aqueous medium by palm bark and sugarcane bagasse: kinetic and thermodynamic study, J. Mater. Environ. Sci., 6 (2015) 2944–2957.
[42] K. Seffah, A. Zafour-Hadj-Ziane, A.T. Achour, J.F. Guillet, P. Lonchambon, E. Flahaut, Adsorption of cadmium ions from water on double-walled carbon nanotubes/iron oxide composite, Chem. J. Mold., 12 (2017) 71–78.
[43] O. Hamdaoui, M. Chiha, Removal of methylene blue from aqueous solutions by wheat bran, Acta Chim. Slov., 54 (2007) 407–418.
[44] İ. Şentürk, M.R. Yıldız, Highly efficient removal from aqueous solution by adsorption of Maxilon Red GRL dye using activated pine sawdust, Korean J. Chem. Eng., 37 (2020) 985–999.
[45] Z. Jiaqi, D. Yimin, L. Danyang, W. Shengyun, Z. Liling, Z. Yi, Synthesis of carboxyl-functionalized magnetic nanoparticle for the removal of methylene blue, Colloids Surf., A, 572 (2019) 58–66.
[46] H.D. Bouras, Z. Isik, E.B. Arikan, A.R. Yeddou, N. Bouras, A. Chergui, L. Favier, A. Amrane, N. Dizge, Biosorption characteristics of methylene blue dye by two fungal biomasses, Int. J. Environ. Stud., 78 (2021) 365–381.
[47] P.D. Shankar, S. Basker, K. Karthik, S. Karthik, D. Centre, N. Arts, N. Arts, Adsorption of methylene blue using passiflora foetida activated carbon on various parameters, Res. J. Chem. Environ. Sci., 5 (2017) 58–66.
[48] C.E. de F. Silva, B.M.V. da Gama, A.H. da S. Gonçalves, J.A. Medeiros, A.K. de S. Abud, Basic-dye adsorption in albedo residue: effect of pH, contact time, temperature, dye concentration, biomass dosage, rotation and ionic strength, J. King Saud Univ. - Eng. Sci., 32 (2020) 351–359.
[49] Y.S. Ho, G. McKay, Kinetic models for the sorption of dye from aqueous solution by wood, Process Saf. Environ. Prot., 76 (1998) 183–191.
[50] S.N. Wang, P. Li, J.J. Gu, H. Liang, J.H. Wu, Carboxylate-functionalized sugarcane bagasse as an effective and renewable adsorbent to remove methylene blue, Water Sci. Technol., 2017 (2018) 300–309.
[51] M.S. Akindolie, H.J. Choi, Surface modification of spent coffee grounds using phosphoric acid for enhancement of methylene blue adsorption from aqueous solution, Water Sci. Technol., 85 (2022) 1218–1234.
[52] H.M. Clark, C.C.C. Alves, A.S. Franca, L.S. Oliveira, Evaluation of the performance of an agricultural residue-based activated carbon aiming at removal of phenylalanine from aqueous solutions, LWT Food Sci. Technol., 49 (2012) 155–161.
[53] Abdullah, E. Alveroğlu Durucu, A. Balouch, A.M. Mahar, Fabrication of silane-modified magnetic nano sorbent for enhanced ultrasonic wave driven removal of methylene blue from aqueous media: isotherms, kinetics, and thermodynamic mechanistic studies, Turk. J. Chem., 45 (2021) 181–191.
[54] Z. Zhang, I.M. O'Hara, G.A. Kent, W.O.S. Doherty, Comparative study on adsorption of two cationic dyes by milled sugarcane bagasse, Ind. Crops Prod., 42 (2013) 41–49.
[55] I.A. Amar, E.A. Zayid, S.A. Dhikeel, M.Y. Najem, Biosorption removal of methylene blue dye from aqueous solutions using phosphoric acid-treated balanites aegyptiaca seed husks powder, Biointerface Res. Appl. Chem., 12 (2022) 7845–7862.
[56] R.A. Akbour, J. El Gaayda, F.E. Titchou, A. Khenifi, H. Afanga, A. Farahi, P.S. Yap, M.B.S. Forte, M. Hamdani, Adsorption of

anionic dyes from aqueous solution using polyelectrolyte pdapdadmac-modified-montmorillonite clay, Desal. Water Treat., 208 (2020) 407–422.
[57] R. Labied, O. Benturki, A.Y. Eddine Hamitouche, A. Donnot, Adsorption of hexavalent chromium by activated carbon obtained from a waste lignocellulosic material (*Ziziphus jujuba* cores): kinetic, equilibrium, and thermodynamic study, Adsorpt. Sci. Technol., 36 (2018) 1066–1099.
[58] S. Kalam, S.A. Abu-Khamsin, M.S. Kamal, S. Patil, Surfactant adsorption isotherms: a review, ACS Omega, 6 (2021) 32342–32348.
[59] M. Belhachemi, F. Addoun, Comparative adsorption isotherms and modeling of methylene blue onto activated carbons, Appl. Water Sci., 1 (2011) 111–117.
[60] G. Annadurai, R.-S. Juang, D.-J. Lee, Use of cellulose-based wastes for adsorption of dyes from aqueous solutions, J. Hazard. Mater., 92 (2002) 263–274.
[61] N. Fayoud, S. Tahiri, S. Alami Younssi, A. Albizane, D. Gallart-Mateu, M.L. Cervera, M. de la Guardia, Kinetic, isotherm and thermodynamic studies of the adsorption of methylene blue dye onto agro-based cellulosic materials, Desal. Water Treat., 57 (2016) 16611–16625.
[62] J. Zhang, Y. Zhou, M. Jiang, J. Li, J. Sheng, Removal of methylene blue from aqueous solution by adsorption on pyrophyllite, J. Mol. Liq., 209 (2015) 267–271.
[63] A. Cemin, F. Ferrarini, M. Poletto, L.R. Bonetto, J. Bortoluz, L. Lemée, R. Guégan, V.I. Esteves, M. Giovanela, Characterization and use of a lignin sample extracted from *Eucalyptus grandis* sawdust for the removal of methylene blue dye, Int. J. Biol. Macromol., 170 (2021) 375–389.
[64] G.L. Dotto, J.M.N. Santos, I.L. Rodrigues, R. Rosa, F.A. Pavan, E.C. Lima, Adsorption of methylene blue by ultrasonic surface modified chitin, J. Colloid Interface Sci., 446 (2015) 133–140.
[65] E.H. Ezechi, S.R.B.M. Kutty, A. Malakahmad, M.H. Isa, Characterization and optimization of effluent dye removal using a new low cost adsorbent: equilibrium, kinetics and thermodynamic study, Process Saf. Environ. Prot., 98 (2015) 16–32.
[66] H. Grabi, W. Lemlikchi, F. Derridj, S. Lemlikchi, M. Trari, Efficient native biosorbent derived from agricultural waste precursor for anionic dye adsorption in synthetic wastewater, Biomass Convers. Biorefin., (2021), doi: 10.1007/s13399-021-01280-9.
[67] H. Sudrajat, A. Susanti, D.K.Y. Putri, S. Hartuti, Mechanistic insights into the adsorption of methylene blue by particulate durian peel waste in water, Water Sci. Technol., 84 (2021) 1774–1792.